IJASRaR
ISSN: 3062-2751

International Journal of Applied Sciences and Radiation Research

Vol. 3-No.1 (2026) pp. 48-53 https://doi.org/10.22399/ijasrar.68

Research Article *www.ijasrar.com*

Exposure Buildup Factor Analysis of $MgO–B_2O_3–SiO_2–La_2O_3$ Glass for Gamma-Ray Shielding Applications

Mazdak Nik-Bakht*

Concordia University-Canada

* **Corresponding Author Email:** mazdak.nikbakht@concordia.ca - **ORCID:** 0000-0003-1705-1093

Article History:

Received: Sep. 02, 2026
Revised: Oct. 28, 2026
Accepted: Oct. 29, 2026

Keywords:

Gamma-ray shielding;
Exposure buildup factor;
Borosilicate glass;
Lanthanum oxide;
Geometric progression method

Abstract: The exposure buildup factor (EBF) is an important parameter in gamma-ray shielding analysis because it accounts for the contribution of scattered photons to the total exposure. This study examines the energy- and penetration-depth dependence of EBF for a magnesium borosilicate glass containing lanthanum oxide, with nominal composition 40MgO–22.5B□O□–30SiO□–7.5La□O□ (mol%) and a reported density of 3.14 g cm□³. The analysis uses the EBF values and geometric-progression (G-P) fitting parameters supplied in the accompanying dataset. The tabulated EBF values cover photon energies from 0.015 to 15 MeV and penetration depths from 0.5 to 40 mean free paths (MFP). The results show that EBF generally increases with penetration depth, demonstrating the increasing contribution of scattered radiation in thicker optical paths. Across most of the investigated range, the largest values occur in the intermediate-energy region: at 10 MFP, the maximum tabulated EBF is 13.993 at 0.8 MeV, while at 40 MFP the maximum among the non-anomalous energy entries is 98.662 at 0.6 MeV. A pronounced outlier occurs at 0.06 MeV, where the EBF rises to 64,605.13 at 40 MFP. Because this value differs markedly from neighboring energy points, it is identified as requiring verification against the original calculation or source database. The study provides a dataset-based description of EBF behavior for the investigated glass; it does not establish comparative shielding superiority or experimental performance.

1. Introduction

The design of radiation-shielding materials requires an understanding of both primary photon attenuation and the secondary radiation generated within the shielding medium. In narrow-beam conditions, attenuation is commonly described by the uncollided photon component. In practical broad-beam geometries, however, photons scattered within the material can also contribute to the exposure measured beyond the shield. The exposure buildup factor (EBF) quantifies this contribution as the ratio of total exposure, including scattered and uncollided photons, to the exposure due to uncollided photons alone [1,3].Glass systems are of interest in radiation protection because their chemical composition can be adjusted by incorporating different oxide constituents. Magnesium borosilicate glasses provide a matrix in which the relative amounts of network-forming and modifying oxides can be varied. Incorporation of lanthanum oxide introduces a heavier constituent into the glass composition. Nevertheless, the shielding implications of a composition must be assessed using clearly defined radiation-interaction quantities and should not be inferred from composition alone.

The geometric-progression (G-P) method is an established approach for representing gamma-ray buildup factors as functions of photon energy and penetration depth. The method uses a set of energy-dependent fitting parameters to estimate buildup factors over a specified range of mean free paths [1,2]. Harima et al. demonstrated the applicability of the G-P representation to buildup-factor data, while later work described its use in shielding calculations across broad energy and depth ranges [1,2]. The radiation shielding properties has been investigated in terms of different parameters in the literatüre [4-18].

The present work analyzes the EBF dataset supplied for $40MgO–22.5B_2O_3–30SiO_2–7.5La_2O_3$ glass. The objective is to describe the variation of EBF with photon energy and penetration depth, identify the regions of comparatively high buildup, and flag any numerical behavior that warrants

The copyright of the published article belongs to its author under CC BY 4.0 license. To view a copy of this licence, visit http://creativecommons.org/licenses/by/4.0/

checking. The analysis is restricted to EBF; energy absorption buildup factors and other attenuation quantities in the workbook are not included in the present discussion.

2. Materials and Methods

2.1. Glass composition and dataset

The investigated composition is reported in the workbook as $40MgO + 22.5B_2O_3 + 30SiO_2 + 7.5La_2O_3$, with Al_2O_3 and Y_2O_3 each listed at 0 mol%. The fraction basis is molar, and the reported density is 3.14 g cm^{-3}. The workbook also lists an average molecular weight of 402.018461 g mol^{-1}. The nominal composition and basic material information are summarized in Table 1.

Table 1. *Nominal composition and reported properties of the investigated glass*.

Parameter	Value	Unit / basis
MgO	40.0	mol%
B_2O_3	22.5	mol%
SiO_2	30.0	mol%
La_2O_3	7.5	mol%
Al_2O_3	0	mol%
Y_2O_3	0	mol%
Density	3.14	g cm^{-3}
Average molecular weight	402.018461	g mol^{-1}

The EBF section of the workbook contains values at 25 photon energies between 0.015 and 15 MeV. For each energy, EBF is tabulated at 0.5, 1, 2, 3, 4, 5, 6, 7, 8, 10, 15, 20, 25, 30, 35, and 40 MFP. The G-P fitting parameters (a, b, c, d, and Xk) are also provided for these energy points. The present analysis uses the tabulated EBF values directly and does not recalculate or independently validate the underlying transport calculations.

2.2. Exposure buildup factor and G-P representation

The exposure buildup factor is defined as:

$$EBF(E, x) = \text{Total exposure} / \text{Uncollided-photon exposure} \quad (1)$$

where E is the incident photon energy and x is the penetration depth expressed in mean free paths. The mean free path is related to the linear attenuation coefficient μ by MFP = 1/μ.
In the G-P method, the buildup factor is expressed as [1,2]:

$$B(E, x) = 1 + (b - 1)\,[K(E, x)^x - 1] / [K(E, x) - 1] \quad (2)$$

with the limiting form $B(E, x) = 1 + (b - 1)x$ when $K(E, x) = 1$. The energy- and depth-dependent parameter K is given by:

$$K(E, x) = c\,x^a + d\,\{\tanh(x/Xk - 2) - \tanh(-2)\} / \{1 - \tanh(-2)\} \quad (3)$$

Here, a, b, c, d, and Xk are the G-P fitting parameters reported in the workbook. The tabulated EBF values are used for the plots and numerical comparisons below. Photon energy is expressed in MeV and penetration depth in MFP.

2.3. Data treatment

The EBF values were organized by photon energy and penetration depth. Energy-dependence comparisons were made at 1, 10, 20, and 40 MFP, while penetration-depth trends were examined for selected energies. Because the value at 0.06 MeV increases sharply at large MFP compared with adjacent energy entries, it is retained in the dataset presentation but explicitly flagged as an outlier requiring source verification. No smoothing, deletion, or correction of this value was performed.

3. Results and Discussions

3.1. Energy dependence of EBF

Figure 1 presents EBF as a function of photon energy at selected penetration depths. At shallow penetration, EBF values are relatively close to unity over much of the low-energy region. For example,

at 1 MFP, the minimum tabulated value is 1.010 at 0.02 MeV, whereas the maximum is 1.854 at 0.5 MeV. The energy dependence is not monotonic: EBF increases toward the intermediate-energy region and then generally decreases at higher energies.
At 10 MFP, the maximum tabulated EBF is 13.993 at 0.8 MeV. The values at 0.5 and 0.6 MeV are 13.123 and 13.788, respectively, indicating a broad region of elevated buildup around 0.5–0.8 MeV. At 20 MFP, the largest non-anomalous value occurs at 0.6 MeV (35.535), closely followed by 0.8 MeV (36.025). These results show that the energy corresponding to the highest EBF can shift with penetration depth.

The overall shape is consistent with the general energy dependence expected for photon buildup: the balance among photon interaction processes changes with energy, influencing the production and transport of scattered photons. The EBF dataset itself does not provide process-resolved contributions, so the present results are interpreted as an observed numerical trend rather than a quantitative decomposition of interaction mechanisms.

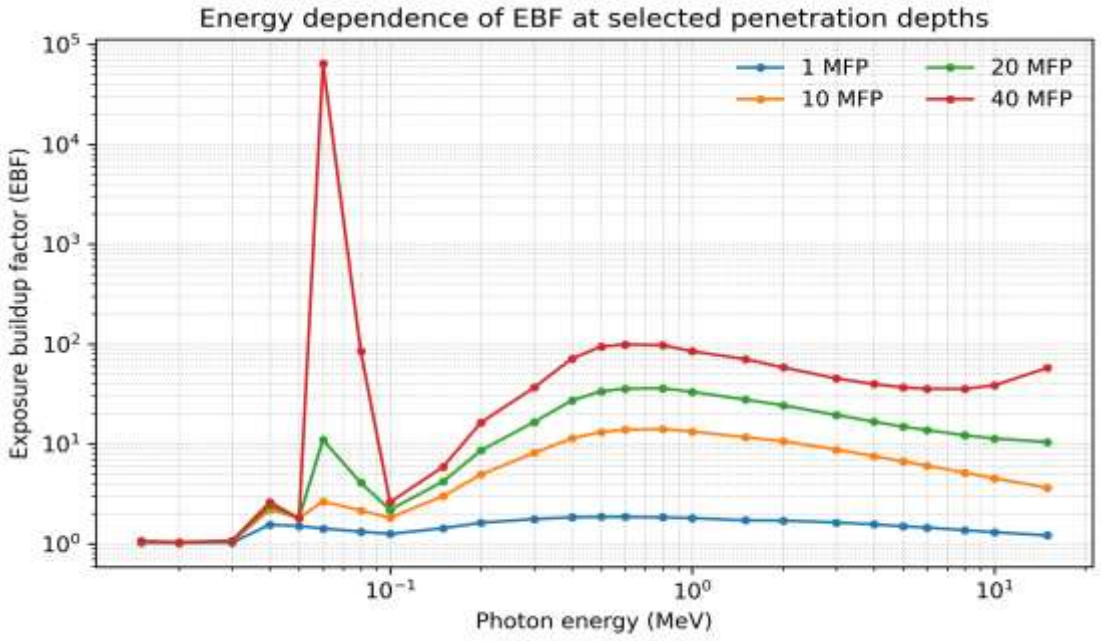

Figure 1. *Exposure buildup factor as a function of photon energy at selected penetration depths. The vertical axis is logarithmic.*

3.2. Dependence on penetration depth

Figure 2 shows the variation of EBF with penetration depth for selected photon energies. For most energies, EBF increases with increasing MFP. This behavior reflects the growing contribution of photons that have undergone one or more scattering events while traversing a greater optical thickness. The magnitude of the increase depends strongly on photon energy.
For example, at 0.8 MeV, EBF increases from 1.397 at 0.5 MFP to 13.993 at 10 MFP and 96.987 at 40 MFP. At 0.6 MeV, the corresponding values are 1.410, 13.788, and 98.662. At 0.02 MeV, by contrast, EBF increases only from 1.008 at 0.5 MFP to 1.021 at 10 MFP and 1.033 at 40 MFP. Thus, the influence of penetration depth is particularly pronounced in the intermediate-energy region.

3.3. Representative EBF values and anomalous entry

Selected values from the supplied EBF table are summarized in Table 2. The table illustrates the increase in buildup with depth and the comparatively high values in the intermediate-energy range. At 40 MFP, the largest value in the supplied dataset is 64,605.13 at 0.06 MeV. This value is several orders of magnitude greater than the values at neighboring energy points: 84.329 at 0.08 MeV and 2.597 at 0.10 MeV. The abrupt variation is not treated as a physical finding without verification. The 0.06 MeV result should be checked against the original G-P parameter source and the calculation procedure, particularly the parameter set and the numerical implementation at large penetration depths. Possible causes cannot be identified from the spreadsheet alone. Until this check is completed, the 0.06 MeV, high-MFP values

should not be used to support a material-performance claim. The data point has been retained in Figure 2 and Table 2 to preserve traceability.

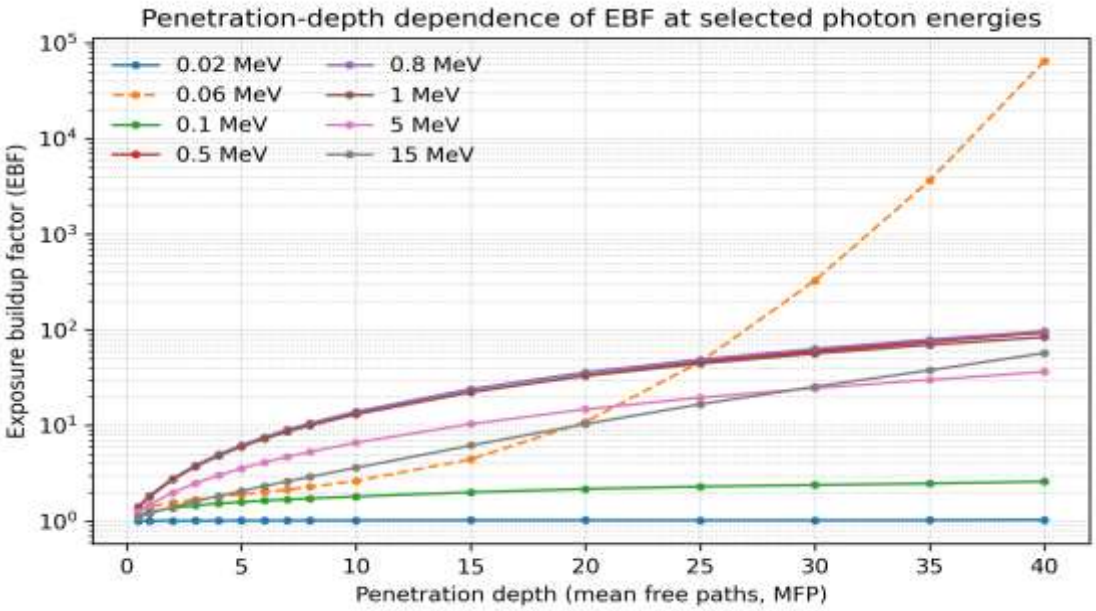

Figure 2. *Exposure buildup factor as a function of penetration depth for selected photon energies. The 0.06 MeV series is shown with a dashed line because of its unusually high values at large MFP.*

Table 2*. Selected exposure buildup factor values extracted from the supplied dataset.*

Energy (MeV)	0.5 MFP	1 MFP	4 MFP	10 MFP	40 MFP
0.020	1.008	1.01	1.014	1.021	1.033
0.060	1.286	1.416	1.794	2.643	6.461e+04
0.080	1.21	1.317	1.63	2.146	84.33
0.100	1.153	1.249	1.532	1.814	2.597
0.500	1.416	1.854	4.892	13.12	93.83
0.600	1.41	1.851	4.996	13.79	98.66
0.800	1.397	1.829	4.98	13.99	96.99
1.000	1.385	1.803	4.822	13.25	84.28
5.000	1.245	1.49	3.017	6.628	36.54
15.000	1.106	1.206	1.835	3.624	57.38

3.4. Implications for shielding assessment

The EBF results demonstrate why buildup should be considered alongside uncollided-photon attenuation in broad-beam shielding calculations. A material can exhibit an energy- and depth-dependent scattered-photon contribution that is not represented by a single attenuation coefficient. For the present glass, the supplied values indicate particularly strong buildup in the intermediate-energy range at large penetration depths. However, EBF alone does not establish the overall shielding effectiveness of a material, because it is a multiplicative correction to uncollided exposure rather than a direct measure of transmitted dose for a specified shield geometry and source.The workbook provides a single glass composition and does not include a comparison with reference materials or experimental measurements. Therefore, no claim of superiority over lead glass, ordinary borosilicate glass, or other shielding materials is made. Future work should verify the anomalous entry, document the calculation code and cross-section library used to generate the EBF parameters, and compare the glass with established shielding materials under identical conditions.

4. Conclusions

The exposure buildup factor of $40MgO–22.5B_2O_3–30SiO_2–7.5La_2O_3$ glass (mol%), with a reported density of 3.14 g cm^{-3}, was analyzed using the EBF values and G-P fitting parameters supplied in the Excel dataset. The tabulated results cover 0.015–15 MeV and 0.5–40 MFP.

The main findings are as follows: (i) EBF generally increases with penetration depth; (ii) the highest non-anomalous values occur in the intermediate-energy region, with a maximum of 13.993 at 0.8 MeV and 10 MFP; (iii) at 40 MFP, the largest non-anomalous value is 98.662 at 0.6 MeV; and (iv) the 0.06 MeV entry reaches 64,605.13 at 40 MFP and requires verification before interpretation. The results provide a dataset-based characterization of EBF for the investigated glass but do not, by themselves, demonstrate experimental shielding performance or superiority over other materials.

Further research should validate the G-P data and calculation methodology, investigate the anomalous low-energy result, and include comparative and experimental assessments.

Author Statements:

- **Ethical approval:** The conducted research is not related to either human or animal use.
- **Conflict of interest:** The authors declare that they have no known competing financial interests or personal relationships that could have appeared to influence the work reported in this paper
- **Acknowledgement:** The authors declare that they have nobody or no-company to acknowledge.
- **Author contributions:** The authors declare that they have equal right on this paper.
- **Funding information:** The authors declare that there is no funding to be acknowledged.
- **Data availability statement:** The data that support the findings of this study are available on request from the corresponding author. The data are not publicly available due to privacy or ethical restrictions.
- **Use of AI Tools:** The author(s) declare that no generative AI or AI-assisted technologies were used in the writing process of this manuscript

References

[1] Harima, Y., Sakamoto, Y., Tanaka, S., & Kawai, M. (1986). Validity of the geometric-progression formula in approximating gamma-ray buildup factors. Nuclear Science and Engineering, 94(1), 24–35. https://doi.org/10.13182/NSE86-A17113

[2] Harima, Y., Tanaka, S., Sakamoto, Y., & Hirayama, H. (1991). Development of new gamma-ray buildup factor and application to shielding calculations. Journal of Nuclear Science and Technology, 28(1), 74–84. https://doi.org/10.1080/18811248.1991.9731324

[3] Harima, Y. (1993). An historical review and current status of buildup factor calculations and applications. Radiation Physics and Chemistry, 41(4–5), 631–672. https://doi.org/10.1016/0969-806X(93)90317-N

[4] Seher Polat, Mucize Sarıhan, Roya Boudaghi Malidarreh3, Sabiha Anas Boussaa, Nurdan Karpuz, & Nuray Kutu. (2026). ANN Prediction of Linear Attenuation Coefficients for 40MgO–30B2O3–30SiO2 System. *International Journal of Applied Sciences and Radiation Research* , *3*(1). https://doi.org/10.22399/ijasrar.56

[5] Lotfihagh, A., & Roya Boudaghi Malidarreh. (2025). FLASH Radiotherapy: Biochemical Mechanisms, Current Evidence, and Remaining Challenges. *International Journal of Biological-Medical Science and Technology*, *3*(1). https://doi.org/10.22399/ijbimes.20

[6] Betul Cetin, & Betul Sezer. (2025). Comparison of the radiation shielding effect of travertine and gasconcrete. *International Journal of Natural-Applied Sciences and Engineering*, *3*(1). https://doi.org/10.22399/ijnasen.31

[7] Waheed, F., Mohamed Abdulhusein Mohsin Al-Sudani, & Iskender Akkurt. (2025). The Experimental Enhancing of the Radiation Shield Properties of Some Produced Compounds. *International Journal of Applied Sciences and Radiation Research* , *2*(1). https://doi.org/10.22399/ijasrar.1

[8] Nasser Khidhr Alhazmi, Sultan Dagham Alanazi, Hammad Shabeeb A Alrowily, Khaled Fayez Alkhamsan, Fawaz Awad Dahisan Al-Rashidi, Al-Salem Sultan Mohammed, … Ahmed Ayyaf k AlQusayri. (2026). Radiation Safety Compliance and Protective Practices Among Radiologic Technologists. *International Journal of Computational and Experimental Science and Engineering*, *10*(4). https://doi.org/10.22399/ijcesen.4664

[9] Demet Sarıyer. (2025). A FLUKA-Based Study on the Effect of Boron-Enhanced Concrete on Secondary Neutron Dose under Proton Beam Loss Scenarios. *International Journal of Natural-Applied Sciences and Engineering*, *3*(1). https://doi.org/10.22399/ijnasen.30

[10] SOYAL, H., & SARIHAN, M. (2025). Radiation Safety Awareness for Future Healthcare Workers: Educational and Legal Perspectives. *International Journal of Biological-Medical Science and Technology*, *3*(1). https://doi.org/10.22399/ijbimes.1

[11] Günoğlu, K., & Akkurt, İskender. (2024). Gamma-ray attenuation properties carbide compounds (WC, Mo2C, TiC, SiC, B4C) using Phy-X/PSD software. *International Journal of Applied Sciences and Radiation Research* , *1*(1), 1–8. https://doi.org/10.22399/ijasrar.6

[12] Demet Sarıyer, & Mustafa Emre Erbil. (2026). Comparative Analysis of Secondary Particle Production and Spatial Dose Distributions in Multilayer Concrete-Iron Shielding Systems for a 50 MeV Proton Accelerator Using FLUKA. *International Journal of Computational and Experimental Science and Engineering*, *12*(1). https://doi.org/10.22399/ijcesen.5083

[13] Sibel ÖZAVCI, & Betül ÇETİN. (2017). Experimental Investigation of Radiation Shielding Effect in Different Doped Slag Concrete. *International Journal of Sustainable Science and Technology*, *2*(1). https://doi.org/10.22399/ijsusat.23

[14] Nuray Kutu. (2026). Radiation Shielding Properties of recycled waste glass color doped powder cement pastes. *International Journal of Applied Sciences and Radiation Research* , *3*(1). https://doi.org/10.22399/ijasrar.55

[15] Sağlam, F., & Cetin, B. (2025). Investigation of Gamma Shielding Properties of Some Industrial Materials. *International Journal of Computational and Experimental Science and Engineering*, *11*(2). https://doi.org/10.22399/ijcesen.1357

[16] Menşure Canpolat, & Halil Soyal. (2025). The Relationship Between Radiation Safety and Ergonomics in Healthcare Workers: Comprehensive Protection Approaches. *International Journal of Biological-Medical Science and Technology*, *3*(1). https://doi.org/10.22399/ijbimes.21

[17] Betul Cetin, Arzu Poyraz, & Melek Gul. (2026). Examination of the radiation absorption parameters of CuO coatings prepared at different ratios. *International Journal of Sustainable Science and Technology*, *4*(1). https://doi.org/10.22399/ijsusat.35

[18] Emikönel, S., & Akkurt, İskender. (2025). Radiation Shielding Properties of B2O3-Bi2O3 Glass . *International Journal of Computational and Experimental Science and Engineering*, *11*(2). https://doi.org/10.22399/ijcesen.2157